

1 **Title**

2 Evaluating the Potential of Full-waveform Lidar for Mapping Pan-Tropical Tree Species Richness

3

4 **Short title**

5 Lidar and Pan-Tropical Tree Species Richness

6

7 **Abstract**

8 **Aim:**

9 Mapping tree species richness across the tropics is of great interest for effective conservation and
10 biodiversity management. In this study, we evaluated the potential of full-waveform lidar data for
11 mapping tree species richness across the tropics by relating measurements of vertical canopy structure,
12 as a proxy for the occupation of vertical niche space, to tree species richness.

13 **Location:**

14 Tropics

15 **Time period:**

16 Present

17 **Major taxa studied:**

18 Trees

Methods:

First, we evaluated the characteristics of vertical canopy structure across 15 study sites using (simulated) large-footprint full-waveform lidar data (22 m diameter) and related these findings to in-situ tree species information. Then, we developed structure-richness models at the local (within 25-50 ha plots), regional (biogeographic regions), and pan-tropical scale at three spatial resolutions (1.0, 0.25 and 0.0625 ha) using Poisson regression.

Results:

The results showed a weak structure-richness relationship at the local scale. At the regional scale (within a biogeographical region) a stronger relationship between canopy structure and tree species richness across different tropical forest types was found, for example across Central Africa and in South America (R^2 ranging from 0.44-0.56, RMSD ranging between 23-61%). Modelling the relationship pan-tropically, across four continents, 39% of the variation in tree species richness could be explained with canopy structure alone ($R^2 = 0.39$ and RMSD = 43%, 0.25 ha resolution).

Main Conclusions:

Our results may serve as a basis for the future development of a set of structure-richness models to map high resolution tree species richness using vertical canopy structure information from the Global Ecosystem Dynamics Investigation (GEDI). The value of this effort would be enhanced by access to a larger set of field reference data for all tropical regions. Future research could also support the use of GEDI data in frameworks using environmental and spectral information for modelling tree species richness across the tropics.

Keywords

Biodiversity, canopy structure, GEDI, lidar, plant area index, tropical forests

1. Introduction

Tropical forests are known for their high tree species diversity. Current estimates suggest in the order of 15,000 tree species in Amazonia alone, in contrast to 124 tree species in temperate forests in Europe, and more than 40,000 different tree species across the tropical region (Slik *et al.*, 2015; Ter Steege *et al.*, 2015). High levels of tree species richness may contribute to maximizing the provision of essential ecosystem services (Liang *et al.*, 2016). Unfortunately, thirty-five percent of pre-agricultural global forest cover has been lost over the past 300 years, largely due to increasing human pressures on the environment. Eighty-two percent of the remaining forest is estimated to have experienced some degree of human impact (Watson *et al.*, 2018). The Convention of Biological Diversity (CBD) and Group on Earth Observations Biodiversity Observation Network (GEO BON) have developed a list of important variables aiming to provide quantitative information on biodiversity to reach the Aichi biodiversity targets 2020 (Pereira *et al.*, 2013; Skidmore *et al.*, 2015). Among the identified needs is the mapping of taxonomic diversity at high spatial resolution over large scales (Pereira *et al.*, 2010). Here we focus on tree species diversity. The collection of tree species diversity data is traditionally done in the field, and such information has previously been used to create predictive maps of tree species richness across the globe at low spatial resolution (Kier *et al.*, 2005; Mutke & Barthlott, 2005). More recently, passive remote sensing data, such as optical imagery from various airborne and spaceborne platforms, has been used in combination with field reference data to predict tree species diversity in different regions (Foody & Cutler, 2006; Carlson *et al.*, 2007; Féret & Asner, 2014; Rocchini *et al.*, 2016; Schäfer *et al.*, 2016; Bongalov *et al.*, 2019). Even though such methods have been developing progressively over the last decade, they are not yet operational for mapping tree species richness across the tropics due to, among others, a lack of consistent remote sensing and training data over such scales, insufficient model accuracy and/or low spatial resolution.

The scientific community has called for bolder science in conservation strategies to enable effective management of the Earth's forests and allow for better conservation of our natural ecosystems (Lewis *et al.*, 2015; Watson *et al.*, 2016). In this study we focus on the use of active remote sensing, specifically lidar, for mapping taxonomic tree species richness in the tropics. While local tropical forest diversity is largely independent of biomass in intact forests (Sullivan *et al.*, 2017), it remains unclear if substantial amounts of variation in species diversity are associated with other features of forest structure. Here, we explore for the first time whether small-scale vertical canopy structure variation is significantly associated with the spatial variation in tropical tree species richness. On a global scale it has previously been shown that canopy height explains a limited portion of the variation in tree species diversity, as such data provide information on the available niche space (Gatti *et al.*, 2017). It has since been hypothesized that including information on the vertical canopy structure, must explain more of the variation in tree species diversity than canopy height alone, as such data provide information on the occupation of the vertical niche space. Marselis *et al.* (2019) demonstrated that information on canopy height and vertical canopy structure, expressed as the Plant Area Index (PAI) profile from full-waveform airborne lidar data, could be used to map tree species diversity in Gabon, Africa. However, it is not clear whether this relationship is of a similar nature and strength across different regions, or even the entire tropics. If existent, then the use of such a structure-diversity relationship(s) could be applied at a pan-tropical scale with the rapidly increasing availability of spaceborne canopy structure information derived from the Global Ecosystem Dynamics Investigation (GEDI), a full-waveform spaceborne lidar system (Dubayah *et al.*, 2020d). GEDI is expected to provide over 10 billion measurements of vertical canopy structure across the temperate and tropical forests between 2019 and 2021.

Factors influencing tree species diversity on a global scale differ from those affecting spatial patterns at regional or local scales. In general, tropical tree species diversity increases with increasing precipitation, forest stature, soil fertility, time since catastrophic disturbance, and rate of canopy turnover; and

decreases with seasonality, latitude, and altitude (Givnish, 1999). At large-grain scales historical biogeographical processes are more important, whereas at the plot-scale environmental variables strongly influence diversity (Keil & Chase, 2019).

Similar to species diversity, forest structure at the global scale is influenced by interacting historic, environmental, and human related variables; precipitation in the wettest month being the most important single predictor of plant height (Moles *et al.*, 2009). Forest structure measured in the field is mainly comprised of four variables: canopy height, biomass, basal area, and tree density (Palace *et al.*, 2015). However, active remote sensing techniques have revolutionized the study of canopy structure (Newnham *et al.*, 2015). With lidar remote sensing, for example, it is now possible to obtain information on canopy height, as well as the position and amount of plant material along the vertical axis of the canopy (Tang *et al.*, 2012). Palace *et al.* (2015) stressed that high resolution lidar data possess vertical structure information which is inherently linked to ecological processes.

We hypothesize that structure-diversity relationships will vary across different biogeographical and phylogenetic regions (Corlett & Primack, 2011; Slik *et al.*, 2018) and that it may be more fruitful to develop multiple relationships rather than one pan-tropical relationship for operationalizing tree species diversity mapping with spaceborne active remote sensing data. Additionally, the strength of the relationship between a variable and tree species diversity often changes with resolution (plot size) as tree species diversity is not linearly related with area (species-area curve) (MacArthur & Wilson, 1967). This complicates the development of predictive models at specific resolutions, and also limits the extrapolation of estimates at one resolution to a larger area, which impedes the mapping of pan-tropical tree species diversity at high spatial resolution.

In sum, we know that both species diversity and canopy structure vary greatly within and across continents. Hence, our objective is to assess whether canopy structure information can explain tree

111 species richness at the local, regional and/or pan-tropical scale with the ultimate goal to evaluate the
112 efficacy of spaceborne full-waveform lidar for mapping tree species richness across the tropics. First, we
113 compare characteristics of the vertical canopy structure, measured with full-waveform lidar data, for
114 tropical forests across the world. Second, we evaluate the differences in species richness and species-
115 area curves across the different study sites using field measurements. Third, we evaluate the potential
116 for developing local (within 25-50 ha field plots), regional (within biogeographical regions) and pan-
117 tropical structure-richness relationships, relating canopy structure metrics from lidar to tree species
118 richness measurements from the field at three spatial resolutions (0.0625, 0.25 and 1.0 ha). Lastly, we
119 discuss the potential of full-waveform lidar data from GEDI for mapping tree species richness across the
120 tropics using structure-richness relationships.

2. Materials and Methods

We address the relationship between canopy structure and tree species richness in *terra firme* forest in the tropical region between 23.5° N and S. We compiled a field and lidar dataset covering colonizing forest, old-growth tropical forest and forests under different degrees of degradation and savanna. We included such a wide variety of forest stages as most of the Earth's tropical forests have been degraded or otherwise affected by natural and human influences (Lewis *et al.*, 2015). Hence, when developing a method that allows for estimating pan-tropical tree species richness it is important to include data covering this range of possibilities.

Species diversity can be expressed with a variety of indicators. Generally, three levels of diversity are recognized: α , β , and γ diversity. α diversity refers to the local diversity of a community, habitat or field plot. β diversity refers to the differences in diversity between habitats and γ diversity to the total diversity of a region (Colwell, 2009). In this study we focus on α diversity. α diversity can be expressed with many different metrics. In this study we focus on one dimension of species diversity: species richness (S) expressed as the total number of species in a plot of a given size. From here on forward we only refer to tree species richness, used to express the local tree species diversity. We chose species richness as it is easy to interpret, and it can probably be used most directly by ecosystem managers. This measure of species diversity is sometimes referred to as species density as it does not consider the number of trees sampled in each plot.

2.1 Field Datasets

Field data were used to calculate the reference values of tree species richness. We used 15 datasets: one from Australia, two from South-East Asia, six from Africa, three from South America and three from Central America (Figure 1). All field datasets used in this study have been previously collected and published and have coincident airborne lidar data available. Each field dataset is labeled with a three-

letter code and contained information on tree location, species, and diameter at breast height (DBH). All datasets were collected by different organizations and research teams resulting in different data characteristics (Table 1, SI1). Four datasets consisted of one large plot of 25 ha (*rob*, Australia and *rab*, Gabon) or 50 ha (*dan*, Malaysia and *bci*, Panama). The other eleven datasets consisted of multiple (3-21) smaller plots with sizes ranging from 0.16 ha to 4.0 ha.

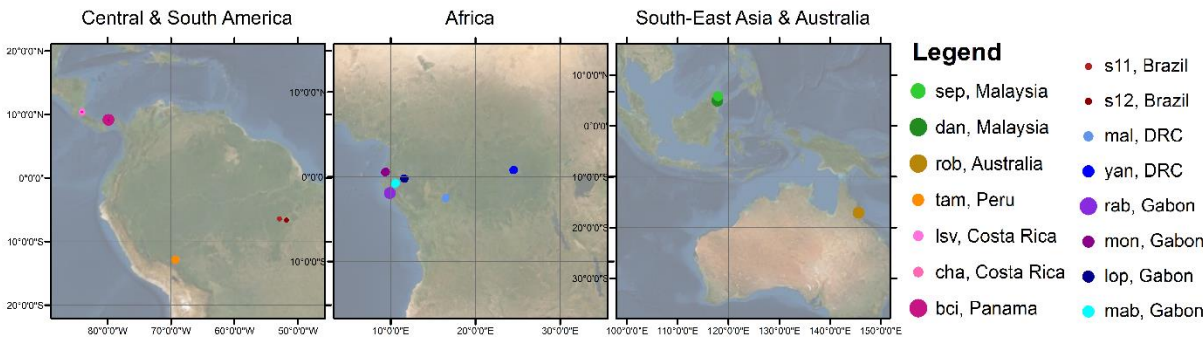


Figure 1: Location of field sites across the three continents, colors of each study site are consistent throughout the paper. Gridlines indicate 10° intervals in longitudinal and latitudinal directions. The size of the place markers represents the size of the total sampled area relative to each other.

Table 1: Information on the original plot size, the amount of total area sampled in the field and the source of the data which is either a website where the data are published and/or a publication in which the data are described further.

Country	Project code	No. native plots	Total area (ha)	Source / Additional Information
Oceania				
Australia	<i>rob</i>	1	25	(Bradford <i>et al.</i> , 2014)
South-East Asia				
Malaysia	<i>dan</i>	1	50	https://forestgeo.si.edu/sites/asia/danum-valley
Malaysia	<i>sep</i>	9	36	https://www.forestplots.net/en/ (Lopez-Gonzalez <i>et al.</i> , 2009, 2011; Jucker <i>et al.</i> , 2018)
Africa				
DRC	<i>mal</i>	21	21	(Bastin <i>et al.</i> , 2015)
DRC	<i>yan</i>	9	9	(Kearsley <i>et al.</i> , 2013)
Gabon	<i>rab</i>	1	25	https://forestgeo.si.edu/sites/africa/rabi (Memiaghe <i>et al.</i> , 2016; Engone Obiang <i>et al.</i> , 2019)
Gabon	<i>lop</i>	11	9.5	https://www.forestplots.net/en/ (Labrière <i>et al.</i> , 2018)
Gabon	<i>mon</i>	12	12	(Fatoyinbo <i>et al.</i> , 2017)
Gabon	<i>mab</i>	10	10	(Bastin <i>et al.</i> , 2015; Labrière <i>et al.</i> , 2018)
South America				
Peru	<i>tam</i>	6	6	https://www.forestplots.net/en/ (Boyd <i>et al.</i> , 2013)
Brazil	<i>s11</i>	8	1.44	http://www.paisagenslidar.cnptia.embrapa.br/webgis/
Brazil	<i>s12</i>	21	3.36	http://www.paisagenslidar.cnptia.embrapa.br/webgis/
Central America				
Costa Rica	<i>lsv</i>	18	9	https://tropicalstudies.org/carbono-project/ (Clark & Clark, 2000)
Costa Rica	<i>cha</i>	3	2	http://neoselvas.wordpress.uconn.edu/costa-rica/
Panama	<i>bci</i>	1	50	https://forestgeo.si.edu/sites/neotropics/barro-colorado-island (Lobo & Dalling, 2013)

157

158 In this study, we assessed the structure-richness relationship at three spatial resolutions (1.0, 0.25,
159 0.0625 ha) because of the non-linear relationship between the number of tree species (*S*) and sampled
160 area. We selected squares of 1.0 ha (100 x 100 m) because they are often-used in ecology and it has
161 been shown that the spatial mismatch of plot location and remote sensing products is minimized at this
162 resolution (Réjou-Méchain *et al.*, 2014). We used squares of 0.25 ha (50 x 50 m) because these yielded
163 the best results describing the structure-diversity relationship in Gabon (Marselis *et al.*, 2019), and
164 squares of 0.0625 ha (25 x 25 m) because they correspond to a resolution close to the GEDI footprint

size. The datasets were used at one, two or three of the aforementioned resolutions depending on the original plot size and the availability of stem maps or subplots (Table 1, full table in SI1). For each of the field sites we calculated S for the entire dataset and for each plot at each plot size (Table 2). Only live trees with a DBH ≥ 10 cm were included, to ensure consistency among datasets, and we included all plots of each resolution in which more than 80% of the trees were identified to at least the genus level.

Table 2: The total number of species identified at each study site and the average (\bar{x}) and standard deviation (s) of the species richness for each of the three plot sizes expressed as $\bar{x} \pm s$ (including only live trees with DBH ≥ 10 cm).

Country	Project Name	Total No. species	Total sampled area used (ha)	Species richness 1.0 ha	Species richness 0.25 ha	Species richness 0.0625 ha
<i>Oceania</i>						
Australia	<i>rob</i>	205	25	98 \pm 10	56 \pm 8	27 \pm 5
<i>South-East Asia</i>						
Malaysia	<i>dan</i>	260	6	117 \pm 13	51 \pm 7	19 \pm 4
Malaysia	<i>sep</i>	517	32	102 \pm 22	53 \pm 11	-
<i>Africa</i>						
DRC	<i>mal</i>	116	21	37 \pm 11	20 \pm 7	-
DRC	<i>yan</i>	232	9	50 \pm 23	24 \pm 13	10 \pm 6
Gabon	<i>rab</i>	234	25	84 \pm 8	42 \pm 6	17 \pm 4
Gabon	<i>lop</i>	118	9.5	32 \pm 22	17 \pm 10	8 \pm 4
Gabon	<i>mon</i>	146	12	32 \pm 15	15 \pm 9	7 \pm 5
Gabon	<i>mab</i>	196	10	55 \pm 8	-	-
<i>South America</i>						
Peru	<i>tam</i>	517	6	171 \pm 13	70 \pm 9	24 \pm 5
Brazil	<i>s11</i>	91	1.44	-	-	17 \pm 3
Brazil	<i>s12</i>	135	3.36	-	-	16 \pm 4
<i>Central America</i>						
Costa Rica	<i>lsv</i>	216	9	-	48 \pm 8	19 \pm 5
Costa Rica	<i>cha</i>	81	2	58	28 \pm 5	13 \pm 4
Panama	<i>bci</i>	220	50	87 \pm 8	42 \pm 6	17 \pm 3

2.2 Lidar Datasets

Each of the field datasets had coincident discrete return airborne laser scanning (ALS) data, or full-waveform lidar data from the Land Vegetation and Ice Sensor (LVIS), collected over the field plots within 5 years of field data collection. We used the GEDI simulator (Hancock *et al.*, 2019) to create lidar

waveforms from the ALS data over the field plots. The ALS data was originally collected with a variety of airborne instruments, but the GEDI simulator ensures a reliable GEDI-like waveform with minimal influence of the original instrument-specific characteristics. In this way, all lidar information could be processed consistently across all study sites ensuring a reliable inter-comparison of canopy structure metrics derived from the waveforms and allowing for easy transfer of the developed models to future on-orbit GEDI data. Lidar waveforms were simulated with a 22 m ground footprint (Gaussian distribution of laser energy, $\sigma = 5.5$ m). Lidar waveform locations were determined by filling each field plot, using the original field plot size and shape, with footprint center locations 6.25 m from the plot edge and 5 m between footprint center locations (Figure 2). This allowed a reliable measure of canopy structure to be acquired for each plot by averaging lidar metrics from all waveforms inside the plot, instead of using single waveforms in the plot center and evaluating structure-richness relationships based on such potentially unrepresentative waveforms. The following information was extracted from each simulated lidar waveform using mature and published algorithms: canopy height (expressed as the 98th percentile of the relative height metric; RH98), total Plant Area Index (PAI), and Plant Area Index at a 1 m vertical resolution (Drake *et al.*, 2002; Tang *et al.*, 2012; Marselis *et al.*, 2018; Hancock *et al.*, 2019). The 1 m vertical profile was used to compare the canopy structure across the study sites. It was aggregated into a 10 m vertical profile, summing all PAI values in each 10 m vertical bin, to be used in the structure-richness analyses. We chose to use the PAI profile because it is a biophysical variable describing the amount of plant material along the vertical forest axis, thus directly indicating the occupation of vertical space. Marselis *et al.*, (2019) previously showed this information relates well to tree species richness in Africa. The average of each of the resulting metrics from all waveforms within each plot was computed to represent the canopy structure for each plot at each spatial resolution.

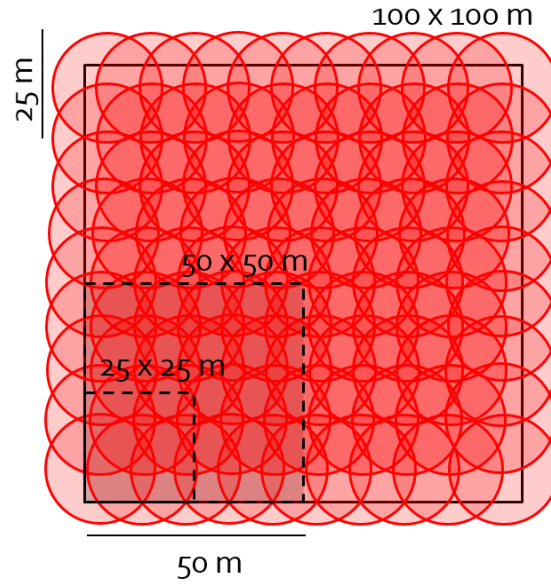


Figure 2: Illustration of simulated lidar waveform layout. The waveforms (red circles) have a Gaussian energy distribution with $\sigma=5.5$ m, resulting in a roughly 22 m diameter footprint. Example of simulated footprint distribution locations in a 1.0 (solid outline), 0.25 and 0.0625 ha field plot (dashed outline). Note: this footprint distribution was chosen to accurately depict canopy structure within the 0.0625, 0.25 and 1.0 ha plots but it does not represent the spatial distribution of spaceborne GEDI waveforms.

2.3 Canopy Structure across the tropics

To evaluate the canopy characteristics across the different study sites we calculated the median plant area volume density profile (composed of the PAI values for each 1 m vertical bin), using all simulated lidar waveforms for each study site. In addition to the median (50th percentile), we calculated the 10th, 30th, 70th and 90th percentiles of the PAI values in the same 1 m vertical bins, to provide a representative distribution of the canopy structure across each study site.

2.4 Species-area relationships across the tropics

We created species-area relationships, calculating the mean and standard deviation of S for plot sizes ranging between 0.01 and 50 ha, to assess how species richness changes by plot size across our study sites. Each of the original field plots was filled with as many non-overlapping subplots as possible at 17 spatial resolutions (0.01, 0.0225, 0.04, 0.09, 0.16, 0.25, 0.36, 0.64, 1.0, 2.25, 4.00, 6.25, 9.00, 12.25, 16.0, 25.0, 50.0 ha) with each tree assigned to a subplot at each resolution. The plot sizes used at each study

site depended on the original plot size and the availability of stem maps (SI1). We visualized the mean and standard deviation of *S* for each plot size at each study site to evaluate the differences in species-area curves across the tropics.

2.5 Structure-Richness Analysis

To evaluate the existence of a relationship between vertical canopy structure and tree species richness across the tropics, we developed models at three scales: local, regional, and pan-tropical, because many historical and environmental drivers of (tree) species diversity have stronger or weaker relations depending on the scale of observation (Gaston, 2000; Keil & Chase, 2019) as do different ecosystem functions (Chisholm *et al.*, 2013). Definitions of the scales are presented in the following sections.

2.5.1 Local Analysis

The local analysis focused on the structure-richness relationship within large (25 or 50 ha) plots. We used data from adjacent field plots to evaluate the relationship between *S* and the canopy structure expressed as canopy height (RH98), total PAI and vertical canopy profile (PAI at 10 m vertical intervals). The local analysis was performed on data collected in *bci* (50 ha), *rab* and *rob* (25 ha). The other 50 ha plot (*dan*) was not suitable for this analysis because the species identification was incomplete at the time of analysis (Table 1). We related the canopy structure with *S* using a generalized linear model with a Poisson error distribution. We used 5-fold cross-validation, extracting 20% of the data at random in each fold as test data. We first performed feature selection on the training data, choosing the model with the lowest Bayesian Information Criterion (BIC) score, and then constructed the predictive model based on the same training data. We evaluated model performance using R^2 , Root Mean Squared Difference as a percentage of the mean (RMSD%) and bias based on the predictions for the test data (Piñeiro *et al.*, 2008). The average and 95% confidence interval of these metrics were recorded for each study site at each resolution.

2.5.2 Regional and Pan-tropical Analysis

The regional analysis was focused on the structure-richness relationship based on non-adjacent plots across study sites within the same biogeographical zone. We evaluated different combinations of study sites at three spatial resolutions (Table 3). To prevent the large plots from dominating the regional and pan-tropical analyses, we thinned their contribution to both the regional and pan-tropical datasets. From the 25 ha plots we selected 1.0 ha plots at each corner, and from the 50 ha plots we selected all corner and the middle plots along the long sides of the plot (6 1.0 ha plots total). To avoid mixing local and regional effects, we employed a Monte-Carlo simulation approach in which we drew different samples from the full regional dataset. In each Monte-Carlo run we randomly sampled one plot at the given resolution from each original plot location (especially important at the 0.25 and 0.0625 ha resolutions at which up to 16 plots exist at the location of each original 1.0 ha plot) and applied a cross-validation (80/20) or leave-one-out cross validation (if $n \leq 25$) approach. In the cross-validation we again performed a two-step approach: first we performed variable selection on the Poisson regression model choosing the model with lowest BIC (using the *bestglm* package in R), and then built the predictive model with the chosen variables. We applied the model to the test data and calculated the model performance statistics for each fold according to Piñeiro *et al.* (2008).

The pan-tropical analysis focused on the structure-richness relationship combining the information from all 15 study sites across all tropical regions, in other words, it was a special case of the regional analysis in which data from all sites was included. Thus, the same methods were applied as in the regional analysis.

261 *Table 3: Number of plots from each dataset used for regional and pan-tropical analysis of the structure-*
262 *richness relationships. Note that one region may not contain the same number of plots across all*
263 *resolutions due to limitations in the availability of subplot and stem map information, limiting the use of*
264 *data from some study sites to only one or two resolutions.*

Region	Resolution (ha)	Study sites															Total
		<i>sep</i>	<i>dan</i>	<i>rob</i>	<i>lsv</i>	<i>cha</i>	<i>bci</i>	<i>tam</i>	<i>s11</i>	<i>s12</i>	<i>mal</i>	<i>yan</i>	<i>rab</i>	<i>mon</i>	<i>lop</i>	<i>mab</i>	
Africa	1										21	9	4	10	8	10	62
	0.25										21	9	4	11	11		56
	0.0625											9	4	12	11		36
South America	1																-
	0.25																-
	0.0625							6	8	21							35
Central America	1																-
	0.25				18	3	6										27
	0.0625				18	3	6										27
South-East Asia	1	9	2														11
	0.25	9	2														11
	0.0625																-
Pan-tropical	1	9	2	4		1	6	6			21	9	4	10	8	10	90
	0.25	9	2	4	18	3	6	6			21	9	4	11	11		104
	0.0625		6	4	18	3	6	6	8	21		9	4	12	11		108

265

266 3. Results

267 3.1 Vertical forest structure across the tropics

268 The vertical canopy structure of forests, in terms of the vertical distribution of plant material varies
269 between tropical regions (Figure 3). Maximum canopy height in our study sites in the Neotropics and
270 Central Africa is typically around 40 m, and slightly lower in Australia, while canopy heights in South-East
271 Asia exceed 60 m. Many sites show a distinct understory layer and a decrease in plant material through
272 the canopy. Relative to the understory, the canopy layer sharply declines in vegetation density (*sep* and
273 *dan*, Malaysia) or steadily declines along the vertical axis (*bci*, Panama; *rab*, Gabon; *mal*, DRC; *rob*,
274 Australia). This vertical distribution of declining vegetation is exacerbated in degraded forests: in *s11*,
275 *s12* (Brazil) and *mon* (Gabon), where the bulk of the vegetation exists close to the forest floor at ~5 m

276 height, but remnant trees in some plots may reach 40 m. Other sites, especially undisturbed ones, have
277 distinct canopy layers. In *tam* (Peru) and in the old-growth forest in *lsv* (Costa Rica) there are multiple
278 peaks of high-density vegetation across the vertical strata of the forest. The profiles of *yan* (DRC) and *lop*
279 (Gabon) are characterized by a multiple-peak pattern, with one peak 20-30 m in the canopy and another
280 within 5 m of the ground, reflecting the inherent structure of the forest-savanna mosaic. The less
281 disturbed *mab* (Gabon) forest shows high variability in canopy structure between plots (e.g. the wide
282 shaded area in Figure 3).

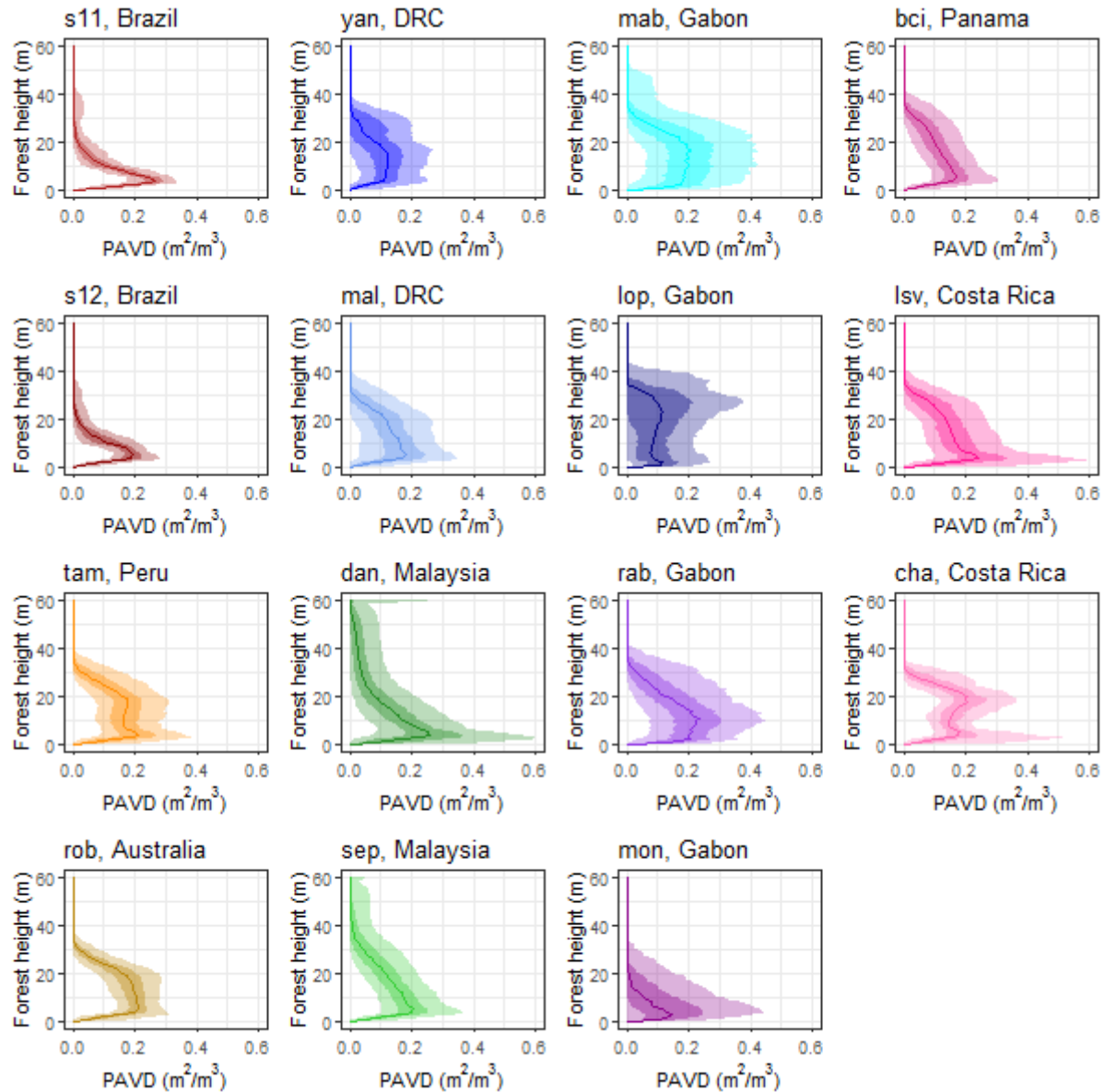


Figure 3: Canopy structure expressed as the Plant Area Volume Density profile (PAVD), expressing the Plant Area Index for each 1 m vertical bin, displayed as the median of all plots within each study site (solid line), the 30th-70th percentile (darker shaded area) and 10th-90th percentile (lighter shaded area).

3.2 Species-area relationships

The number of species increases with plot size, but the rate of increase varies across study sites (Figure 4). For example, in *rob* (Australia) 82-117 species occur in a 1.0 ha plot compared to 16-44 species in 0.0625 ha plots. By contrast, *tam* (Peru) contains 154-185 species/ha, but only 11-35 species in a 0.0625

ha plot, similar to *rob*. Thus, species' composition of adjacent 0.0625 ha plots in *tam* must be more dissimilar from each other than adjacent 0.0625 ha plots in *rob* (Australia), in other words, the β diversity of the plots in *tam* is higher than in *rob*. The species-area curves vary in shape across study sites, with the highest total species richness in *tam* and lowest species richness in the African sites (Figure 4). Curves that are initially steep and decrease in slope at larger plot sizes indicate a high α diversity but a lower β diversity (e.g. when the area is increased, the same species are encountered).

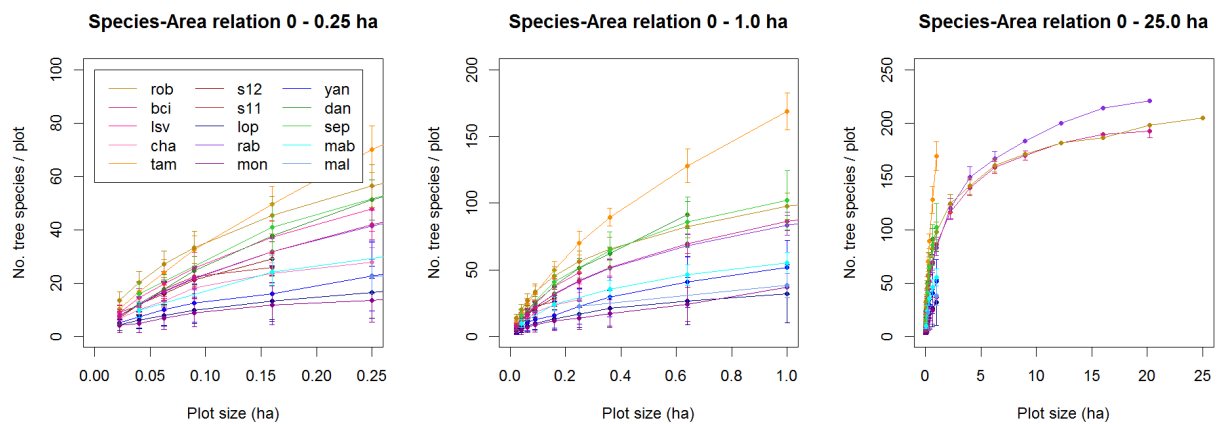


Figure 4: Relationships between tree species richness and area for each study site (note the change in y-axis across panels from left to right).

3.3 Structure-richness relationships

Pulling together the information on tree species richness and canopy structure (RH98 and Total PAI), species richness generally increases with increasing canopy height and increasing total Plant Area Index across the tropics (Figure 5).

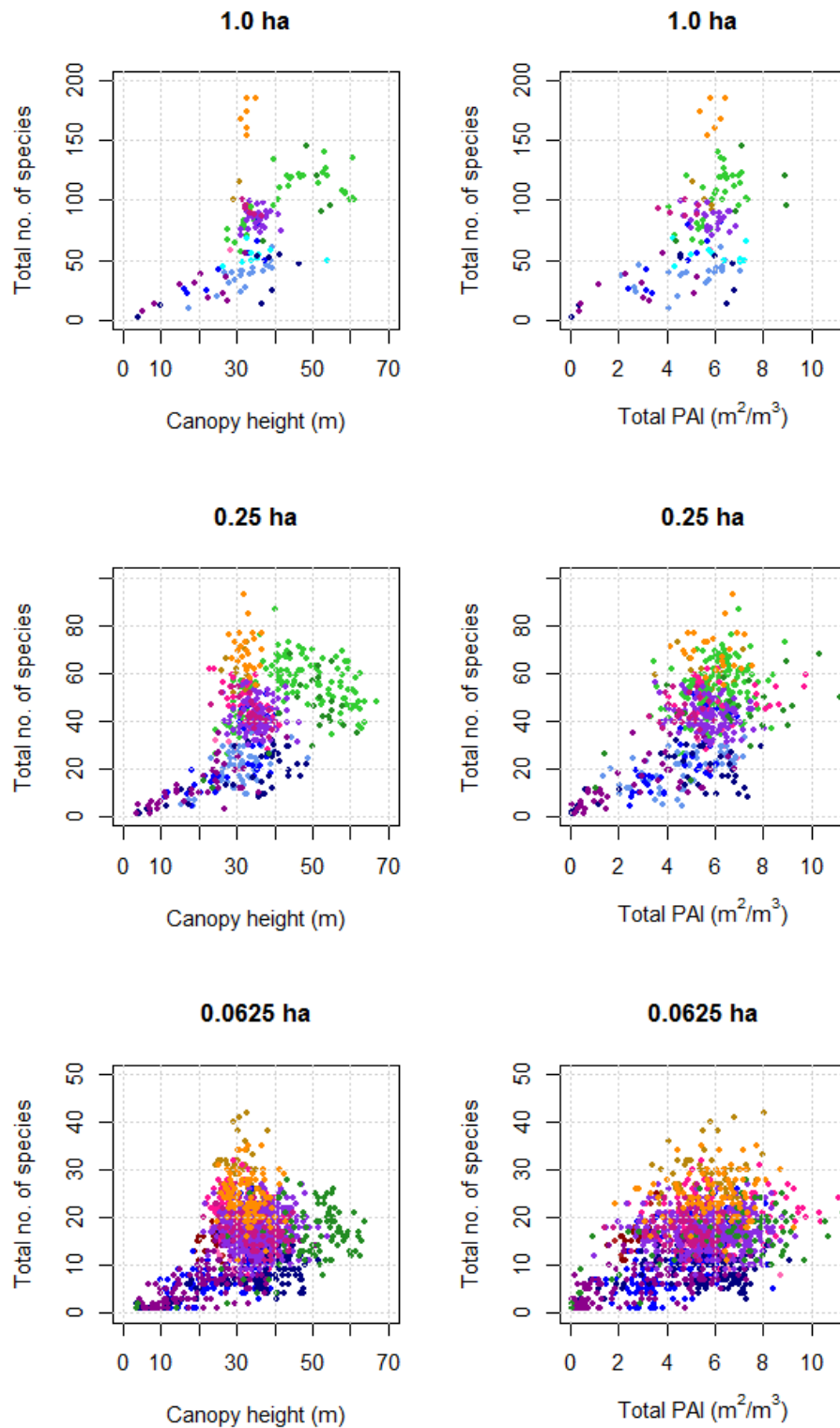


Figure 5: Relation between canopy height (left) and total PAI (right) across three spatial scales for all study sites across the tropics. Each point represents one plot at the specific resolution. Dots are colored by study site corresponding according to legend in Figure 1.

310 The cross-validation results of the local models reveal weak structure-richness relationships. Of the
311 three large plots (25 and 50 ha), only the models for *bci* (50 ha) show evidence of a significant
312 relationship between the predicted and observed values ($R^2=0.32$ at 1.0 ha, SI2). Even though species
313 richness within all three large plots can be predicted with a root mean squared error between 7-20% of
314 the mean species richness, the low RMSD% found only indicates that the predictions at the local scale
315 are close to the mean species richness, however in *rab* and *rob* the canopy structure is insensitive to the
316 local variation in tree species richness (see for example Figure SI2-1).

317 Regional structure-richness models generally show much better performance (Figure 6) than the local
318 models in terms of the variance in species richness that can be explained with the canopy structure
319 information (mostly significant models and higher R^2 values). However, prediction error (as percentage
320 of the mean species richness) is generally higher, partly due to the larger range in species richness in
321 these regional datasets. Regions of Africa and South America (Table 3) show the best model
322 performance whereas regions including the Costa Rica datasets show much poorer performance
323 (regions indicated with *centralamerica*). Results from an additional analysis on the compositional
324 similarity (Bray-Curtis; Faith *et al.*, 1987, SI3) of the Costa Rica dataset showed that, even though species
325 richness varies in Costa Rica (Table 2), the plots share many species, i.e. the composition is similar. In the
326 *africa* and *southamerica* datasets the variation in species richness is accompanied by a much larger
327 variation in species composition (SI3). The variation of the model performance for *seasia* is very high
328 because of the low number of plots available for this region and at the 0.25 ha resolution it was not
329 possible to create a significant model >95% of the Monte-Carlo iterations (Table 3). The model
330 performance does not provide clear results on the effect of the different resolutions, given the
331 overlapping error bars for models in the same region at multiple resolutions and the inability to create
332 each regional model at each spatial resolution (Figure 6).

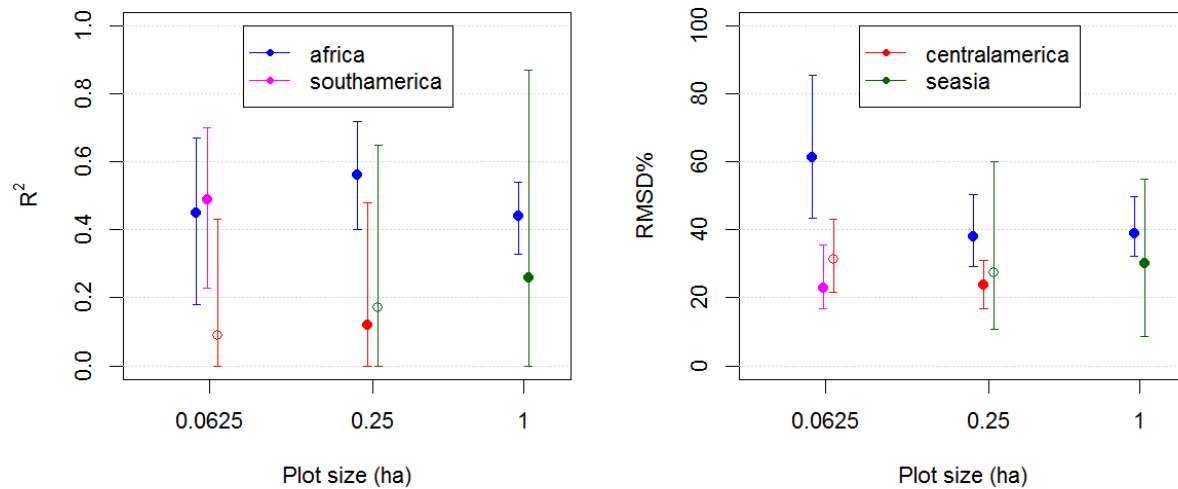


Figure 6: Cross-validated model performance of regional structure-richness models. Error bars indicate the 95% range of values for each performance metric. Solid dots indicate >95% of the generated models was statistically significant, open circles indicate a lower percentage was significant.

Pan-tropical structure-richness models show varying performance across the spatial resolutions with mean R^2 ranging between 0.25 and 0.39 and RMSD% between 66 and 43% for the plot sizes from 1.0 and 0.0625 ha (Figure 7). However, the error bars of the model performance at different resolutions are overlapping, indicating that no resolution has a statistically better performance. Around 39% of the variation in tree species richness can be explained using canopy structure metrics alone at the 0.25 ha resolution at the pan-tropical scale. Sites with extremely high values of observed species richness are generally predicted poorly (SI4).

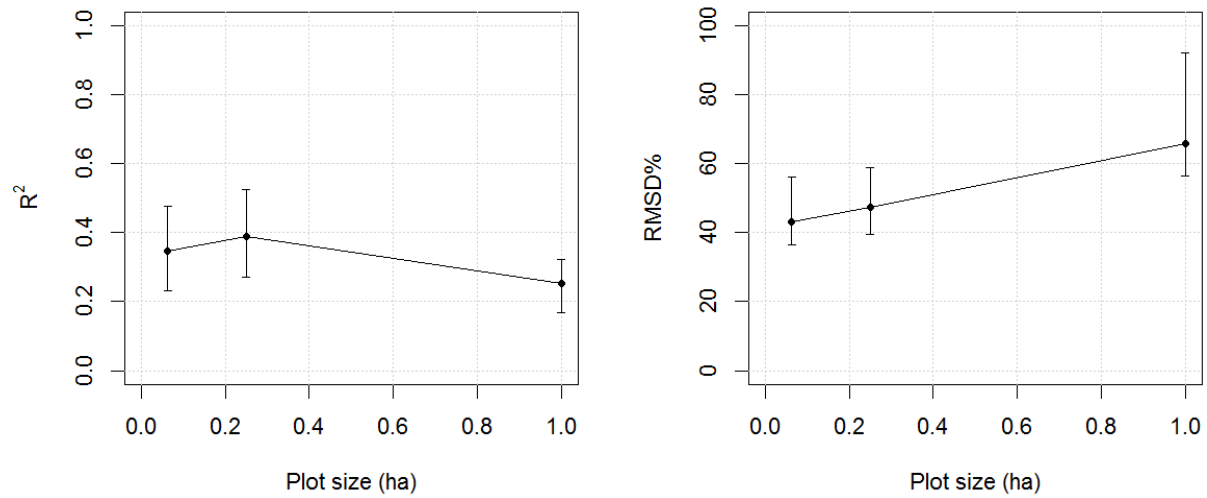


Figure 7: Cross-validated model performance at the pan-tropical scale in terms of R^2 and RMSD%. Error bars indicate the range between which 95% of the performance values of the cross-validated models fall.

4. Discussion

4.1 Structure-richness relationships across scales

In this study we explored the relationships between vertical canopy structure and tree species richness at different resolutions across local, regional and pan-tropical scales, using a total of 15 study sites with coincident lidar and field data across the tropics. We found weak relationships between canopy structure and tree species richness at the local scale and the strongest relationship at the regional scales in Africa and South America. We also found significant relationships between canopy structure and tree species richness combining the data from all study sites across the tropics.

At the local scale, within one large plot inside one forest type, the variation in the canopy structure is determined mostly by variability in growth structure within the same species (the 25 and 50 ha plots have a similar composition throughout the plot, SI1 and SI3). For example, an adult tree of species X may range in height from 20-40 m, so even though the canopy structure may differ between two plots of similar composition, the difference is not attributed to a difference in species composition. Furthermore, if a 20 m and 40 m tree of species X exist in the same plot, due to the difference in canopy structure the model may predict a species richness of 2 based on variation in structure. On the other hand, as area increases it is more likely that the difference in structure is caused by a difference in composition. Do keep in mind that structure can also change due to other variables such as topography, soil, and microclimate. Individuals of most tropical forest species are spatially aggregated (Condit *et al.*, 2000) so the composition of two adjacent plots is more similar than the composition of two more distant plots. This is the case for *bci*, where a 50 ha area with a species richness gradient was sampled (Fricker *et al.*, 2015) and included in the local analysis, which led to more successful prediction of species richness based on structure. Within the 25 ha plots sampled at *rab* and *rob*, the variation in composition is smaller and no significant structure-richness relationships were found (SI3).

Increasing the scale, we found that regions consisting of sites exhibiting a large variation in species composition among plots, but with a similar biogeographical history, show a much stronger structure-richness relationship. However, we note that model performance differed quite drastically across regions. The forest in *Isv*, Costa Rica, consists of largely similar species composition, whereas species composition is much more varied in regions where the structure-richness models perform better (South-America, Africa), supporting the result from local scale models that species richness can be better predicted from canopy structure in areas with greater β diversity.

At the pan-tropical scale we find a significant relationship between canopy structure and tree species richness across all spatial resolutions. At the intermediate resolution (0.25 ha) this relationship appears to be slightly stronger than at the higher and lower resolutions, but no significant difference was found. However, the observed difference may be attributed to the lower sensitivity of species richness to rare species at smaller plot sizes. For example, *tam* (Peru) plots have very high species richness at the 1.0 ha resolution (Table 2), whereas at the 0.0625 ha resolution the species richness ranges between 11-35 species, which is still higher than most other sites but much less than at the 1.0 ha plot size. Because the 1.0 ha plot size captures more rare species in each plot, the 1.0 ha pan-tropical model predictions for *tam* contain highly erroneous predictions that are not present in 0.0625 ha models (SI4). Rare species do not contribute much to the canopy structure, thereby complicating the relationship between structure and richness at a scale at which they contribute largely to species richness numbers.

4.2 Limitations

This research could be significantly improved by using more coincident lidar and field data to thoroughly evaluate the existence and strength of the structure-richness relationship across all tropical regions. However, the collection of such data is costly and time-consuming. Here, we were able to exploit 15 independently collected datasets (SI1), but data gaps exist, especially in the Amazon basin, high biomass

395 forests of Central Africa, the mainland of South-East Asia, New Guinea and Australia as well as the dry
396 tropics and montane ecosystems. Apart from the spatial representation problem, the low number of
397 plots for certain regions likely influences the observed variability in model performance. The pan-
398 tropical models (with $n \geq 90$) show more stable performance than models of regions with low numbers
399 of plots (e.g. *seasia*). A training dataset that does not fully represent the range of structure in the full
400 dataset can lead to biased predictions for some of the test plots. Such errors are exacerbated by the
401 logarithmic link model in Poisson regression because errors can increase exponentially. Even so,
402 negative predictions are possible with linear regression and the risk of underestimating tree species
403 richness is higher for diverse areas. Hence, we chose to use Poisson regression, knowing that it may lead
404 to extreme predictions in some cases that should be accounted for when operationalizing this method.

405 Species diversity can be identified in many different ways (Gotelli & Colwell, 2001; Colwell, 2009) and
406 there are risks and pitfalls using just one metric. In this study we only used 'species richness' (S), defined
407 by the number of different tree species in a defined area (the plot, with different sizes), as this metric is
408 easy to interpret and a prediction of the number of species/area can probably be used most directly by
409 ecosystem managers. Hereby we did not control for the number of stems in the plot, nor for the
410 abundance of the different species. Such information can be considered, for example, by using the
411 Shannon diversity index or rarefaction curves. Moreover, depending on the type of metric, a different
412 model may need to be selected to describe the structure-richness relationship as different metrics are
413 related differently to canopy structure information. For example, a generalized linear regression with a
414 Poisson error distribution, as used here, is more suitable for estimated tree species richness as this is
415 count data, whereas a linear model with a Gaussian error distribution will be better suited for estimating
416 Shannon diversity. Hence, we chose to focus on one metric of diversity to test the structure-richness
417 relationships, while acknowledging other metrics may provide better, worse, or more useful predictions
418 of tree species diversity and these should be considered in the future.

419 This study serves as a first attempt to study the pan-tropical structure-richness relationship and should
420 be improved and further developed when more data become available. Additionally, the characteristics
421 of each dataset differed widely because all data were collected by different researchers and institutions.
422 We accounted for this as much as possible by using datasets only at reliable plot and subplot
423 resolutions, including only trees ≥ 10 cm DBH and including only plots with less than 20% of unidentified
424 trees at the genus level. Nonetheless, we acknowledge that the quality of the species identification
425 varied and may have affected our models as species identification in the tropics can be challenging due
426 to the vast variety of tree species and the fact that new species are still encountered. Species
427 identification of new and existing data could be improved using more botanists or genetic tests in the
428 lab, which has been done for some of the datasets used here, but is not yet feasible for all datasets.
429 Additionally, including information on species for trees with DBH ≥ 10 cm omits large diversity found in
430 the understory. Fricker *et al.* (2015) showed that especially this diversity variation in small trees related
431 well to the canopy structure. Future research should examine if these findings are consistent across the
432 tropics.

433 The availability of stem maps and subplots in each study site determined the spatial resolutions at which
434 datasets could be used. This resulted in the inclusion of different datasets for each region (Table 3). This
435 makes the comparison of model performance in the same region at different resolutions unreliable
436 because the models were not always built on the same data (plots and study sites), but we weighed this
437 decision to maximize the sizes of the datasets used to build the structure-richness models. Hence, no
438 conclusion can be drawn about the optimal resolution for the structure-richness relationships.

439 Accurate geolocation of field plots is key for the development of reliable species-richness models
440 (Fricker *et al.*, 2015). However, geolocation of field plots in the tropical forest can be challenging due to
441 difficulties receiving a reliable GPS signal under dense canopy. This should be taken into account,

especially when evaluating the performance of models build with small field plots, where the effects of such geolocation errors will be larger (Réjou-Méchain *et al.*, 2014).

We included data from a range of forest stages, including old-growth forest, successional stages, disturbed forest and even low tree density savanna sites. The relationships we found are partially driven by this gradient (Figure 5). However, we deemed it essential to include data from across this range of forest types, because if this method is to be operationalized using canopy structure information from across the tropics, we will encounter all these different stages of forest (Lewis *et al.*, 2015). We acknowledge that climatic, edaphic, and topographic variables could also impact tree species richness across the tropics, such as mean annual temperature and precipitation (Keil & Chase, 2019) and slope and elevation (Robinson *et al.*, 2018). However, in this study we specifically focused on the relation between canopy structure and tree species diversity, in light of the recently launched GEDI mission. We recognize that including such information on topographic and environmental variables may further improve the mapping of tree species richness across the tropics.

4.3 Future research & Applications

Our results provide confidence regarding the existence of regional and pan-tropical structure-richness relationships that may be used to map pan-tropical tree species richness. The most accurate predictions seem to be achieved at the regional scale when adequate data are available and when forested areas are grouped by regions of similar biogeographical history. However, in the absence of such data it may be of more immediate interest to further develop pan-tropical models that were shown to explain up to 39% of variation in tree species richness. At the time of writing, GEDI is collecting canopy structure information close to the finest resolution tested here (0.0625 ha) and thus these data may be well suited for mapping tree species richness across the tropics. GEDI is a sampling mission in which lidar waveforms with 25 m diameter footprints are collected across 8 tracks with 600 m between-track

spacing, 60 m along-track spacing (Figure 8). By the end of its nominal two-year mission, GEDI will have sampled roughly 4% of total land area.

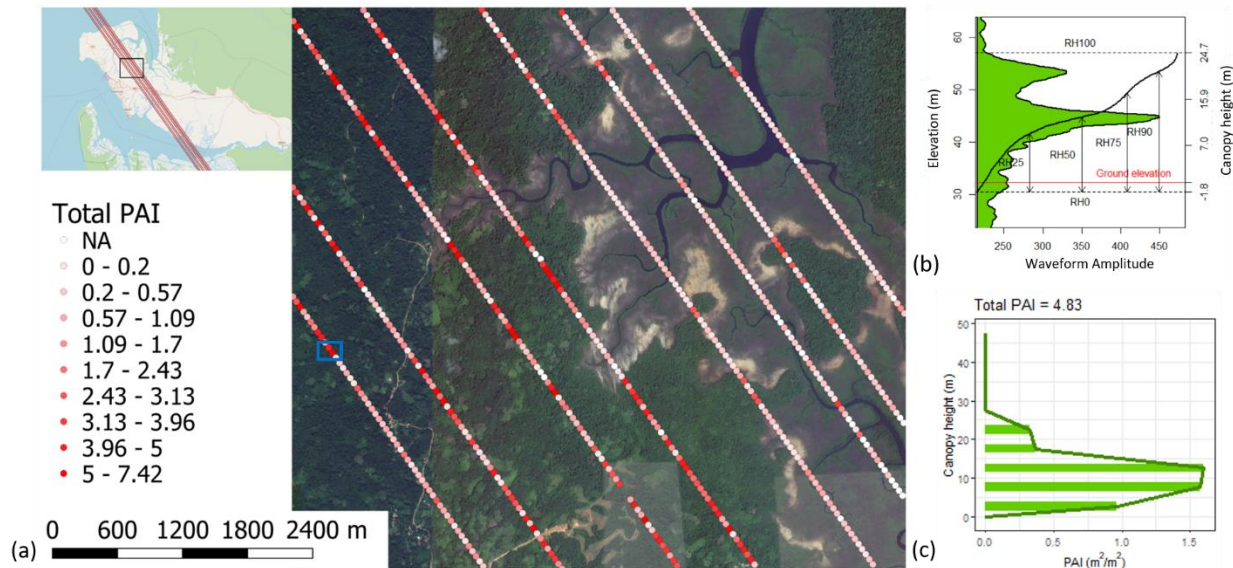


Figure 8: (a) Example of GEDI data captured over the east of Mondah forest, north-west of Libreville, in Gabon, Africa. The lidar waveforms are collected along-track with 8 tracks, a between-track spacing of 600 m and an along-track spacing of 60 m. (b) shows an example GEDI waveform with Relative Height metrics (shot number = 31151116800411054, orbit = 03115, track = 05633); at the location indicated with the blue box on (a)). (c) shows the accompanying PAI profile at 5 m vertical intervals from the Level-2 data product.

The footprint-level GEDI information on vertical canopy structure is stored in the Level-2 data products which are publicly available from the NASA Land Processes Distributed Active Archive Center (LPDAAC)¹ (Dubayah *et al.*, 2020b, a,c). GEDI gridded data products will have a 1 km² or finer resolution (Dubayah *et al.*, 2020d). Our local scale models show that predictions of adjacent 0.0625 ha plots (or in the future, footprints) are on average correct, but they will not detect local nuances in species richness within forests of uniform composition. We suggest that the species richness predictions could potentially be used in a similar way as gridded GEDI data products by estimating the average number of species/0.0625 ha within a 1 km² cell, as such information may still be of interest to local land managers.

¹ <https://lpdaac.usgs.gov/>

Given the variable species-area relationships, it is not easy to translate species richness predictions at 0.0625 ha resolution to the expected number of tree species in 1 km². Also, the amount of variance in species richness explained is limited. Therefore, we propose two future research avenues of interest: fusion with spectral and/or radar data and using an environmental framework. Both spectral data and radar data have previously been shown to predict some of the variance in tree species richness (Foody & Cutler, 2006; Wolf *et al.*, 2012; Schäfer *et al.*, 2016; Bae *et al.*, 2019; Bongalov *et al.*, 2019; Marselis *et al.*, 2019) and may improve our models and allow for more accurate predictions of tree species richness across the tropics and the creation of wall-to-wall data products at higher spatial resolution. Especially data from the hyperspectral HISUI (Matsunaga *et al.*, 2013) instrument, that is soon to be launched to the International Space Station, the radar BIOMASS mission (Le Toan *et al.*, 2011), the ICESat-2 mission (Duncanson *et al.*, 2020) the TanDEM-X mission (Qi *et al.*, 2019) and Landsat (Saarela *et al.*, 2018), may be highly relevant for such applications. Alternatively, we believe that the inclusion of structural data within previously developed environmental and biogeographical frameworks will help to predict tree species diversity (Keil & Chase, 2019) as such frameworks already display intrinsic differences in tree species diversity. Such frameworks could benefit from GEDI lidar data providing information on the occupation of the vertical niche space and likely improve predictions of tree species richness across the tropics, which could then be compared to existing predictions such as from Slik *et al.* (2015). Moreover, it has previously been shown that lidar data can provide interesting information about the diversity of other taxa as well (Huang *et al.*, 2014; Rappaport *et al.*, 2020) and future avenues for using lidar data to provide information on a holistic measure of species diversity, including many taxa, could be of incredible value.

5. Conclusions

In this study we evaluated the existence of local, regional and pan-tropical relationships between vertical canopy structure and tree species richness in the tropics at three spatial resolutions: 1.0, 0.25, and 0.0625 ha. Full-waveform lidar data provides detailed information on the differences in vertical canopy structure between forests across the tropics. Our results show that canopy structure can explain a significant percentage of variation in tree species richness across different biogeographical regions. A full set of regional structure-richness models will most likely aid accurate pan-tropical species richness mapping, but the development of such a set of models is contingent on the availability of sufficient coincident field & lidar data across the tropics. Using one single predictive model at a pan-tropical scale, 39% of the variation in tree species richness could be explained using the vertical canopy structure. Given this canopy structure is measured directly from GEDI waveforms at the footprint level, this provides an interesting avenue for mapping tree species richness at high spatial resolution. Alternatively, canopy structure information from GEDI could be included in existing modeling frameworks, combining structural with spectral, environmental and topographic information to create more accurate tree species richness predictions.

519 References

- 520 Bae, S., Levick, S.R., Heidrich, L., Magdon, P., Leutner, B.F., Wollauer, S., Serebryanyk, A., Nauss, T.,
 521 Krzystek, P., Gossner, M.M., Schall, P., Heibl, C., Bassler, C., Doerfler, I., Schulze, E., Krah, F.,
 522 Culmsee, H., Jung, K., Heurich, M., Fischer, M., Seibold, S., Thorn, S., Gerlach, T., Hothorn, T.,
 523 Weisser, W.W. & Muller, J. (2019) Radar vision in the mapping of forest biodiversity from space.
 524 *Nature Communications*, **10**, 4757.
- 525 Bastin, J.F., Barbier, N., Réjou-Méchain, M., Fayolle, A., Gourlet-Fleury, S., Maniatis, D., De Haulleville, T.,
 526 Baya, F., Beeckman, H., Beina, D., Couteron, P., Chuyong, G., Dauby, G., Doucet, J.L., Droissart, V.,
 527 Dufrêne, M., Ewango, C., Gillet, J.F., Gonmadje, C.H., Hart, T., Kavali, T., Kenfack, D., Libalah, M.,
 528 Malhi, Y., Makana, J.R., Pélissier, R., Ploton, P., Serckx, A., Sonké, B., Stevart, T., Thomas, D.W., De
 529 Cannière, C. & Bogaert, J. (2015) Seeing Central African forests through their largest trees. *Scientific*
 530 *Reports*, **5**.
- 531 Bongalov, B., Burslem, D.F.R.P., Jucker, T., Thompson, S.E.D., Rosindell, J., Swinfield, T., Nilus, R.,
 532 Clewley, D., Phillips, O.L. & Coomes, D.A. (2019) Reconciling the contribution of environmental and
 533 stochastic structuring of tropical forest diversity through the lens of imaging spectroscopy. *Ecology*
 534 *Letters*, **22**, 1608–1619.
- 535 Boyd, D.S., Hill, R.A., Hopkinson, C. & Baker, T.R. (2013) Landscape-scale forest disturbance regimes in
 536 southern Peruvian Amazonia. *Ecological Applications*, **23**, 1588–1602.
- 537 Bradford, M.G., Metcalfe, D.J., Ford, A., Liddell, M.J. & McKeown, A. (2014) Floristics, stand structure
 538 and aboveground biomass of a 25-ha rainforest plot in the wet tropics of Australia. *Journal of*
 539 *Tropical Forest Science*, **26**, 543–553.
- 540 Carlson, K.M., Asner, G.P., Hughes, R.F., Ostertag, R. & Martin, R.E. (2007) Hyperspectral remote sensing
 541 of canopy biodiversity in Hawaiian lowland rainforests. *Ecosystems*, **10**, 536–549.
- 542 Chisholm, R.A., Muller-Landau, H.C., Abdul Rahman, K., Bebbler, D.P., Bin, Y., Bohlman, S.A., Bourg, N.A.,
 543 Brinks, J., Bunyavejchewin, S., Butt, N., Cao, H., Cao, M., Cárdenas, D., Chang, L.W., Chiang, J.M.,
 544 Chuyong, G., Condit, R., Dattaraja, H.S., Davies, S., Duque, A., Fletcher, C., Gunatilleke, N.,
 545 Gunatilleke, S., Hao, Z., Harrison, R.D., Howe, R., Hsieh, C.F., Hubbell, S.P., Itoh, A., Kenfack, D.,
 546 Kiratiprayoon, S., Larson, A.J., Lian, J., Lin, D., Liu, H., Lutz, J.A., Ma, K., Malhi, Y., McMahon, S.,
 547 Mcshea, W., Meegaskumbura, M., Mohd. Razman, S., Morecroft, M.D., Nytch, C.J., Oliveira, A.,
 548 Parker, G.G., Pulla, S., Punchi-Manage, R., Romero-Saltos, H., Sang, W., Schurman, J., Su, S.H.,
 549 Sukumar, R., Sun, I.F., Suresh, H.S., Tan, S., Thomas, D., Thomas, S., Thompson, J., Valencia, R.,
 550 Wolf, A., Yap, S., Ye, W., Yuan, Z. & Zimmerman, J.K. (2013) Scale-dependent relationships between
 551 tree species richness and ecosystem function in forests. *Journal of Ecology*, **101**, 1214–1224.
- 552 Clark, D.B. & Clark, D.A. (2000) Landscape-scale variation in forest structure and biomass in a tropical
 553 rain forest. *Forest ecology and management*, **137**, 185–198.
- 554 Colwell, R.K. (2009) *Biodiversity: concepts, patterns and measurement. The Princeton guide to ecology*,
 555 pp. 257–263.
- 556 Condit, R., Ashton, P.S., Baker, P., Bunyavejchewin, S., Gunatilleke, S., Gunatilleke, N., Hubbell, S.P.,
 557 Foster, R.B., Itoh, A., LaFrankie, J. V., Lee, H.S., Losos, E., Manokaran, N., Sukumar, R. & Yamakura,
 558 T. (2000) Spatial patterns in the distribution of tropical tree species. *Science*, **288**, 1414–1418.

559 Corlett, R.T. & Primack, R.B. (2011) *Tropical Rain Forests: An Ecological and Biogeographical*
560 *Comparison: Second Edition*, 2nd edn. Blackwell Publishing.

561 Drake, J.B., Dubayah, R.O., Knox, R.G., Clark, D.B. & Blair, J.B. (2002) Sensitivity of large-footprint lidar to
562 canopy structure and biomass in a neotropical rainforest. *Remote Sensing of Environment*, **81**, 378–
563 392.

564 Dubayah, R., Hofton, M., Blair, J.B., Armston, J., Tang, H. & Luthcke, S. (2020a) GEDI L2A Elevation and
565 Height Metrics Data Global Footprint Level V001 [Data set].

566 Dubayah, R., Luthcke, S., Blair, J.B., Hofton, M., Armston, J. & Tang, H. (2020b) GEDI L1B Geolocated
567 Waveform Data Global Footprint Level V001 [Data set].

568 Dubayah, R., Tang, H., Armston, J., Luthcke, S., Hofton, M. & Blair, J.B. (2020c) GEDI L2B Canopy Cover
569 and Vertical Profile Metrics Data Global Footprint Level V001 [Data set].

570 Dubayah, R.O., Blair, J.B., Goetz, S., Fatoyinbo, L., Hansen, M., Healey, S., Hofton, M., Hurtt, G., Kellner,
571 J., Luthcke, S., Armston, J., Tang, H., Duncanson, L., Hancock, S., Jantz, P., Marselis, S., Patterson, P.,
572 Qi, W. & Silva, C. (2020d) The Global Ecosystem Dynamics Investigation: High-resolution laser
573 ranging of the Earth's forests and topography. *Science of Remote Sensing*, **1**.

574 Duncanson, L., Neuenschwander, A., Hancock, S., Thomas, N., Fatoyinbo, T., Simard, M., Silva, C.A.,
575 Armston, J., Luthcke, S.B., Hofton, M., Kellner, J.R. & Dubayah, R. (2020) Biomass estimation from
576 simulated GEDI, ICESat-2 and NISAR across environmental gradients in Sonoma County, California.
577 *Remote Sensing of Environment*, **242**, 111779.

578 Engone Obiang, N.L., Kenfack, D., Picard, N., Lutz, J.A., Bissiengou, P., Memiaghe, H.R. & Alonso, A.
579 (2019) Determinants of spatial patterns of canopy tree species in a tropical evergreen forest in
580 Gabon. *Journal of Vegetation Science*, **20**.

581 Faith, D.P., Minchin, P.R. & Belbin, L. (1987) Compositional dissimilarity as a robust measure of
582 ecological distance. *Vegetatio*, **69**, 57–68.

583 Fatoyinbo, T.E., Pinto, N., Simard, M., Armston, J., Duncanson, L., Hofton, M., Saatchi, S., Laval, M.,
584 Lou, Y., Denbina, M., Dubayah, R., Marselis, S.M., Tang, H., Hancock, S. & Hensley, S. (2017) The
585 2016 NASA AfriSAR campaign: airborne SAR and Lidar measurements of tropical forest structure
586 and biomass in support of future satellite missions. *IEEE Journal of Selected Topics in Applied Earth*
587 *Observations and Remote Sensing*, 4286–4287.

588 Féret, J.B. & Asner, G.P. (2014) Mapping tropical forest canopy diversity using high-fidelity imaging
589 spectroscopy. *Ecological Applications*, **24**, 1289–1296.

590 Foody, G.M. & Cutler, M.E.J. (2006) Mapping the species richness and composition of tropical forests
591 from remotely sensed data with neural networks. *Ecological Modelling*, **195**, 37–42.

592 Fricker, G.A., Wolf, J. a., Saatchi, S.S. & Gillespie, T.W. (2015) Predicting spatial variations of tree species
593 richness in tropical forests from high resolution remote sensing. *Ecological Applications*, **25**,
594 150218095111005.

595 Gaston, K.J. (2000) Global patterns in biodiversity. *Nature*, **405**, 220–227.

596 Gatti, R.C., Di Paola, A., Bombelli, A., Noce, S. & Valentini, R. (2017) Exploring the relationship between
597 canopy height and terrestrial plant diversity. *Plant Ecology*, **218**, 899–908.

598 Givnish, T.J. (1999) On the causes of gradients in tropical tree diversity. *Journal of Ecology*, **87**, 193–210.

599 Gotelli, N.J. & Colwell, R.K. (2001) Quantifying biodiversity: procedures and pitfalls in the measurement
600 and comparison of species richness. *Ecology Letters*, **4**, 379–391.

601 Hancock, S., Armston, J., Hofton, M., Sun, X., Tang, H., Duncanson, L.I., Kellner, J.R. & Dubayah, R. (2019)
602 The GEDI Simulator: A Large-Footprint Waveform Lidar Simulator for Calibration and Validation of
603 Spaceborne Missions. *Earth and Space Science*, **6**, 294–310.

604 Huang, Q.Y., Swatantran, A., Dubayah, R. & Goetz, S.J. (2014) The Influence of Vegetation Height
605 Heterogeneity on Forest and Woodland Bird Species Richness across the United States. *Plos One*, **9**,
606 10.

607 Jucker, T., Asner, G.P., Dalponte, M., Brodrick, P.G., Philipson, C.D., Vaughn, N.R., Arn Teh, Y., Brelsford,
608 C., Burslem, D.F.R.P., Deere, N.J., Ewers, R.M., Kvasnica, J., Lewis, S.L., Malhi, Y., Milne, S., Nilus, R.,
609 Pfeifer, M., Phillips, O.L., Qie, L., Renneboog, N., Reynolds, G., Riutta, T., Struebig, M.J., Svátek, M.,
610 Turner, E.C. & Coomes, D.A. (2018) Estimating aboveground carbon density and its uncertainty in
611 Borneo’s structurally complex tropical forests using airborne laser scanning. *Biogeosciences*, **15**,
612 3811–3830.

613 Kearsley, E., De Haulleville, T., Hufkens, K., Kidimbu, A., Toirambe, B., Baert, G., Huygens, D., Kebede, Y.,
614 Defourny, P., Bogaert, J., Beeckman, H., Steppe, K., Boeckx, P. & Verbeeck, H. (2013) Conventional
615 tree height-diameter relationships significantly overestimate aboveground carbon stocks in the
616 Central Congo Basin. *Nature Communications*, **4**.

617 Keil, P. & Chase, J.M. (2019) Global patterns and drivers of tree diversity integrated across a continuum
618 of spatial grains. *Nature Ecology and Evolution*, **3**, 390.

619 Kier, G., Mutke, J., Dinerstein, E., Ricketts, T.H., Küper, W., Kreft, H. & Barthlott, W. (2005) Global
620 patterns of plant diversity and floristic knowledge. *Journal of Biogeography*, **32**, 1107–1116.

621 Labrière, N., Tao, S., Chave, J., Scipal, K., Le Toan, T., Abernethy, K., Alonso, A., Barbier, N., Bissengou, P.,
622 Casal, T. & others (2018) In Situ Reference Datasets From the TropiSAR and AfriSAR Campaigns in
623 Support of Upcoming Spaceborne Biomass Missions. *IEEE Journal of Selected Topics in Applied*
624 *Earth Observations and Remote Sensing*, 1–11.

625 Lewis, S.L., Edwards, D.P. & Galbraith, D. (2015) Increasing human dominance of tropical forests.
626 *Science*, **349**.

627 Liang, J., Crowther, T.W., Picard, N., Wiser, S., Zhou, M., Alberti, G., Schulze, E.D., McGuire, A.D.,
628 Bozzato, F., Pretzsch, H., De-Miguel, S., Paquette, A., Hérault, B., Scherer-Lorenzen, M., Barrett,
629 C.B., Glick, H.B., Hengeveld, G.M., Nabuurs, G.J., Pfautsch, S., Viana, H., Vibrans, A.C., Ammer, C.,
630 Schall, P., Verbyla, D., Tchebakova, N., Fischer, M., Watson, J. V., Chen, H.Y.H., Lei, X., Schelhaas,
631 M.J., Lu, H., Gianelle, D., Parfenova, E.I., Salas, C., Lee, E., Lee, B., Kim, H.S., Bruelheide, H., Coomes,
632 D.A., Piotto, D., Sunderland, T., Schmid, B., Gourlet-Fleury, S., Sonké, B., Tavani, R., Zhu, J., Brandl,
633 S., Vayreda, J., Kitahara, F., Searle, E.B., Neldner, V.J., Ngugi, M.R., Baraloto, C., Frizzera, L., Bałazy,
634 R., Oleksyn, J., Zawila-Niedźwiecki, T., Bouriaud, O., Bussotti, F., Finér, L., Jaroszewicz, B., Jucker, T.,
635 Valladares, F., Jagodzinski, A.M., Peri, P.L., Gonmadje, C., Marthy, W., O’Brien, T., Martin, E.H.,
636 Marshall, A.R., Rovero, F., Bitariho, R., Niklaus, P.A., Alvarez-Loayza, P., Chamuya, N., Valencia, R.,
637 Mortier, F., Wortel, V., Engone-Obiang, N.L., Ferreira, L. V., Odeke, D.E., Vasquez, R.M., Lewis, S.L.
638 & Reich, P.B. (2016) Positive biodiversity-productivity relationship predominant in global forests.
639 *Science*.

640 Lobo, E. & Dalling, J.W. (2013) Effects of topography, soil type and forest age on the frequency and size
641 distribution of canopy gap disturbances in a tropical forest. *Biogeosciences*, **10**, 6769–6781.

642 Lopez-Gonzalez, G., Lewis, S.L., Burkit, M. & Phillips, O.L. (2011) ForestPlots.net: a web application and
643 research tool to manage and analyse tropical forest plot data. *Journal of Vegetation Science*, **22**,
644 610–613.

645 Lopez-Gonzalez, G., Lewis, S.L., Burkitt, M., Baker, T.R. & Phillips, O.L. (2009) ForestPlots.net database.
646 *www.forestplots.net*, Date of Extraction [01,12,17].

647 MacArthur, R.H. & Wilson, E.O. (1967) *The theory of Island Biogeography*, Princeton University Press,
648 Princeton and Oxford.

649 Marselis, S.M., Tang, H., Armston, J., Abernethy, K., Alonso, A., Barbier, N., Bissiengou, P., Jeffery, K.,
650 Kenfack, D., Labrière, N. & others (2019) Exploring the relation between remotely sensed vertical
651 canopy structure and tree species diversity in Gabon. *Environmental Research Letters*, **14**.

652 Marselis, S.M., Tang, H., Armston, J.D., Calders, K., Labrière, N. & Dubayah, R. (2018) Distinguishing
653 vegetation types with airborne waveform lidar data in a tropical forest-savanna mosaic: A case
654 study in Lopé National Park, Gabon. *Remote Sensing of Environment*, **216**, 626–634.

655 Matsunaga, T., Iwasaki, A., Tsuchida, S., Tanii, J., Kashimura, O., Nakamura, R., Yamamoto, H.,
656 Tachikawa, T. & Rokugawa, S. (2013) *Current status of Hyperspectral Imager Suite (HISUI)*.
657 *International Geoscience and Remote Sensing Symposium (IGARSS)*,.

658 Memiaghe, H.R., Lutz, J.A., Korte, L., Alonso, A. & Kenfack, D. (2016) Ecological Importance of Small-
659 Diameter Trees to the Structure, Diversity and Biomass of a Tropical Evergreen Forest at Rabi,
660 Gabon. *PLoS ONE*, **11**.

661 Moles, A.T., Warton, D.I., Warman, L., Swenson, N.G., Laffan, S.W., Zanne, A.E., Pitman, A., Hemmings,
662 F.A. & Leishman, M.R. (2009) Global patterns in plant height. *Journal of Ecology*, **97**, 923–932.

663 Mutke, J. & Barthlott, W. (2005) Patterns of vascular plant diversity at continental to global scales.
664 *Biologische skrifter*, **55**, 521–531.

665 Newnham, G.J., Armston, J.D., Calders, K., Disney, M.I., Lovell, J.L., Schaaf, C.B., Strahler, A.H. & Danson,
666 F.M. (2015) Terrestrial laser scanning for plot-scale forest measurement. *Current Forestry Reports*,
667 **1**, 239–251.

668 Palace, M.W., Sullivan, F.B., Ducey, M.J., Treuhaft, R.N., Herrick, C., Shimbo, J.Z. & Mota-E-Silva, J. (2015)
669 Estimating forest structure in a tropical forest using field measurements, a synthetic model and
670 discrete return lidar data. *Remote Sensing of Environment*, **161**, 1–11.

671 Pereira, H.M., Ferrier, S., Walters, M., Geller, G.N., Jongman, R.H.G., Scholes, R.J., Bruford, M.W.,
672 Brummitt, N., Butchart, S.H.M., Cardoso, A.C., Coops, N.C., Dulloo, E., Faith, D.P., Freyhof, J.,
673 Gregory, R.D., Heip, C., Höft, R., Hurtt, G., Jetz, W., Karp, D.S., McGeoch, M.A., Obura, D., Onoda,
674 Y., Pettorelli, N., Reyers, B., Sayre, R., Scharlemann, J.P.W., Stuart, S.N., Turak, E., Walpole, M. &
675 Wegmann, M. (2013) Essential biodiversity variables. *Science*, **339**, 277–278.

676 Pereira, H.M., Leadley, P.W., Proenca, V., Alkemade, R., Scharlemann, J.P.W., Fernandez-Manjarres, J.F.,
677 Araujo, M.B., Balvanera, P., Biggs, R., Cheung, W.W.L., Chini, L., Cooper, H.D., Gilman, E.L.,
678 Guenette, S., Hurtt, G.C., Huntington, H.P., Mace, G.M., Oberdorff, T., Revenga, C., Rodrigues, P.,
679 Scholes, R.J., Sumaila, U.R. & Walpole, M. (2010) Scenarios for Global Biodiversity in the 21st

680 Century. *Science*, **330**, 1496–1501.

681 Piñeiro, G., Perelman, S., Guerschman, J.P. & Paruelo, J.M. (2008) How to evaluate models: Observed vs.
682 predicted or predicted vs. observed? *Ecological Modelling*, **216**, 316–322.

683 Qi, W., Saarela, S., Armston, J., Stahl, G. & Dubayah, R. (2019) Forest biomass estimation over three
684 distinct forest types using TanDEM-X InSAR data and simulated GEDI lidar data. *Remote Sensing of*
685 *Environment*, **232**.

686 Rappaport, D.I., Royle, J.A. & Morton, D.C. (2020) Acoustic space occupancy: Combining ecoacoustics
687 and lidar to model biodiversity variation and detection bias across heterogeneous landscapes.
688 *Ecological Indicators*, **113**.

689 Réjou-Méchain, M., Muller-Landau, H.C., Detto, M., Thomas, S.C., Le Toan, T., Saatchi, S.S., Barreto-Silva,
690 J.S., Bourg, N.A., Bunyavejchewin, S., Butt, N., Brockelman, W.Y., Cao, M., Cárdenas, D., Chiang,
691 J.M., Chuyong, G.B., Clay, K., Condit, R., Dattaraja, H.S., Davies, S.J., Duque, A., Esufali, S., Ewango,
692 C., Fernando, R.H.S., Fletcher, C.D., N. Gunatilleke, I.A.U., Hao, Z., Harms, K.E., Hart, T.B., Hérault,
693 B., Howe, R.W., Hubbell, S.P., Johnson, D.J., Kenfack, D., Larson, A.J., Lin, L., Lin, Y., Lutz, J.A.,
694 Makana, J.R., Malhi, Y., Marthens, T.R., Mcewan, R.W., McMahon, S.M., Mcshea, W.J., Muscarella,
695 R., Nathalang, A., Noor, N.S.M., Nytch, C.J., Oliveira, A.A., Phillips, R.P., Pongpattananurak, N.,
696 Punchi-Manage, R., Salim, R., Schurman, J., Sukumar, R., Suresh, H.S., Suwanvecho, U., Thomas,
697 D.W., Thompson, J., Uriarte, M., Valencia, R., Vicentini, A., Wolf, A.T., Yap, S., Yuan, Z., Zartman,
698 C.E., Zimmerman, J.K. & Chave, J. (2014) Local spatial structure of forest biomass and its
699 consequences for remote sensing of carbon stocks. *Biogeosciences*, **11**, 6827–6840.

700 Robinson, C., Saatchi, S., Clark, D., Hurtado Astaiza, J., Hubel, A.F. & Gillespie, T.W. (2018) Topography
701 and Three-Dimensional Structure Can Estimate Tree Diversity along a Tropical Elevational Gradient
702 in Costa Rica. *Remote Sensing*, **10**, 629.

703 Rocchini, D., Boyd, D.S., Féret, J.B., Foody, G.M., He, K.S., Lausch, A., Nagendra, H., Wegmann, M. &
704 Pettorelli, N. (2016) Satellite remote sensing to monitor species diversity: potential and pitfalls.
705 *Remote Sensing in Ecology and Conservation*, **2**, 25–36.

706 Saarela, S., Holm, S., Healey, S.P., Andersen, H.E., Petersson, H., Prentius, W., Patterson, P.L., Næsset, E.,
707 Gregoire, T.G. & Ståhl, G. (2018) Generalized hierarchical model-based estimation for aboveground
708 biomass assessment using GEDI and landsat data. *Remote Sensing*.

709 Schäfer, E., Heiskanen, J., Heikinheimo, V. & Pellikka, P. (2016) Mapping tree species diversity of a
710 tropical montane forest by unsupervised clustering of airborne imaging spectroscopy data.
711 *Ecological Indicators*, **64**, 49–58.

712 Skidmore, A.K., Pettorelli, N., Coops, N.C., Geller, G.N., Hansen, M., Lucas, R., Mucher, C.A., O'Connor, B.,
713 Paganini, M., Pereira, H.M., Schaepman, M.E., Turner, W., Wang, T.J. & Wegmann, M. (2015) Agree
714 on biodiversity metrics to track from space. *Nature*, **523**, 403–405.

715 Slik, J.W.F., Arroyo-Rodríguez, V., Aiba, S.-I., Alvarez-Loayza, P., Alves, L.F., Ashton, P., Balvanera, P.,
716 Bastian, M.L., Bellingham, P.J., van den Berg, E., Bernacci, L., da Conceição Bispo, P., Blanc, L.,
717 Böhning-Gaese, K., Boeckx, P., Bongers, F., Boyle, B., Bradford, M., Brearley, F.Q., Breuer-
718 Ndoundou Hockemba, M., Bunyavejchewin, S., Calderado Leal Matos, D., Castillo-Santiago, M.,
719 Catharino, E.L.M., Chai, S.-L., Chen, Y., Colwell, R.K., Chazdon, R.L., Clark, C., Clark, D.B., Clark, D.A.,
720 Culmsee, H., Damas, K., Dattaraja, H.S., Dauby, G., Davidar, P., DeWalt, S.J., Doucet, J.-L., Duque, A.,
721 Durigan, G., Eichhorn, K.A.O., Eisenlohr, P. V., Eler, E., Ewango, C., Farwig, N., Feeley, K.J., Ferreira,

722 L., Field, R., de Oliveira Filho, A.T., Fletcher, C., Forshed, O., Franco, G., Fredriksson, G., Gillespie, T.,
 723 Gillet, J.-F., Amarnath, G., Griffith, D.M., Grogan, J., Gunatilleke, N., Harris, D., Harrison, R., Hector,
 724 A., Homeier, J., Imai, N., Itoh, A., Jansen, P.A., Joly, C.A., de Jong, B.H.J., Kartawinata, K., Kearsley,
 725 E., Kelly, D.L., Kenfack, D., Kessler, M., Kitayama, K., Kooyman, R., Larney, E., Laumonier, Y.,
 726 Laurance, S., Laurance, W.F., Lawes, M.J., Amaral, I.L. do, Letcher, S.G., Lindsell, J., Lu, X., Mansor,
 727 A., Marjokorpi, A., Martin, E.H., Meilby, H., Melo, F.P.L., Metcalfe, D.J., Medjibe, V.P., Metzger, J.P.,
 728 Millet, J., Mohandass, D., Montero, J.C., de Morisson Valeriano, M., Mugerwa, B., Nagamasu, H.,
 729 Nilus, R., Ochoa-Gaona, S., Onrizal, Page, N., Parolin, P., Parren, M., Parthasarathy, N., Paudel, E.,
 730 Permana, A., Piedade, M.T.F., Pitman, N.C.A., Poorter, L., Poulsen, A.D., Poulsen, J., Powers, J.,
 731 Prasad, R.C., Puyravaud, J.-P., Razafimahaimodison, J.-C., Reitsma, J., dos Santos, J.R., Roberto
 732 Spironello, W., Romero-Saltos, H., Rovero, F., Rozak, A.H., Ruokolainen, K., Rutishauser, E., Saiter,
 733 F., Saner, P., Santos, B.A., Santos, F., Sarker, S.K., Satdichanh, M., Schmitt, C.B., Schöngart, J.,
 734 Schulze, M., Suganuma, M.S., Sheil, D., da Silva Pinheiro, E., Sist, P., Stevart, T., Sukumar, R., Sun, I.-
 735 F., Sunderland, T., Suresh, H.S., Suzuki, E., Tabarelli, M., Tang, J., Targhetta, N., Theilade, I., Thomas,
 736 D.W., Tchouto, P., Hurtado, J., Valencia, R., van Valkenburg, J.L.C.H., Van Do, T., Vasquez, R.,
 737 Verbeeck, H., Adekunle, V., Vieira, S.A., Webb, C.O., Whitfeld, T., Wich, S.A., Williams, J., Wittmann,
 738 F., Wöll, H., Yang, X., Adou Yao, C.Y., Yap, S.L., Yoneda, T., Zahawi, R.A., Zakaria, R., Zang, R., de
 739 Assis, R.L., Garcia Luize, B. & Venticinque, E.M. (2015) An estimate of the number of tropical tree
 740 species. *Proceedings of the National Academy of Sciences*, **112**, 7472–7477.

741 Slik, J.W.F., Franklin, J., Arroyo-Rodríguez, V., Field, R., Aguilar, S., Aguirre, N., Ahumada, J., Aiba, S.I.,
 742 Alves, L.F., Anitha, K., Avella, A., Mora, F., Aymard, G.A.C., Báez, S., Balvanera, P., Bastian, M.L.,
 743 Bastin, J.F., Bellingham, P.J., Van Den Berg, E., Da Conceição Bispo, P., Boeckx, P., Boehning-Gaese,
 744 K., Bongers, F., Boyle, B., Brambach, F., Brearley, F.Q., Brown, S., Chai, S.L., Chazdon, R.L., Chen, S.,
 745 Chhang, P., Chuyong, G., Ewango, C., Coronado, I.M., Cristóbal-Azkarate, J., Culmsee, H., Damas, K.,
 746 Dattaraja, H.S., Davidar, P., DeWalt, S.J., Din, H., Drake, D.R., Duque, A., Durigan, G., Eichhorn, K.,
 747 Eler, E.S., Enoki, T., Ensslin, A., Fandohan, A.B., Farwig, N., Feeley, K.J., Fischer, M., Forshed, O.,
 748 Garcia, Q.S., Garkoti, S.C., Gillespie, T.W., Gillet, J.F., Gonmadje, C., Granzow-De La Cerda, I.,
 749 Griffith, D.M., Grogan, J., Hakeem, K.R., Harris, D.J., Harrison, R.D., Hector, A., Hemp, A., Homeier,
 750 J., Hussain, M.S., Ibarra-Manríquez, G., Hanum, I.F., Imai, N., Jansen, P.A., Joly, C.A., Joseph, S.,
 751 Kartawinata, K., Kearsley, E., Kelly, D.L., Kessler, M., Killeen, T.J., Kooyman, R.M., Laumonier, Y.,
 752 Laurance, S.G., Laurance, W.F., Lawes, M.J., Letcher, S.G., Lindsell, J., Lovett, J., Lozada, J., Lu, X.,
 753 Lykke, A.M., Bin Mahmud, K., Mahayani, N.P.Di., Mansor, A., Marshall, A.R., Martin, E.H., Matos,
 754 D.C.L., Meave, J.A., Melo, F.P.L., Mendoza, Z.H.A., Metali, F., Medjibe, V.P., Metzger, J.P., Metzker,
 755 T., Mohandass, D., Munguía-Rosas, M.A., Muñoz, R., Nurtjahya, E., De Oliveira, E.L., Onrizal,
 756 Parolin, P., Parren, M., Parthasarathy, N., Paudel, E., Perez, R., Pérez-García, E.A., Pommer, U.,
 757 Poorter, L., Qi, L., Piedade, M.T.F., Pinto, J.R.R., Poulsen, A.D., Poulsen, J.R., Powers, J.S., Prasad,
 758 R.C., Puyravaud, J.P., Rangel, O., Reitsma, J., Rocha, Di.S.B., Rolim, S., Rovero, F., Rozak, A.,
 759 Ruokolainen, K., Rutishauser, E., Rutten, G., Mohd Said, M.N., Saiter, F.Z., Saner, P., Santos, B., Dos
 760 Santos, J.R., Sarker, S.K., Schmitt, C.B., Schoengart, J., Schulze, M., Sheil, D., Sist, P., Souza, A.F.,
 761 Spironello, W.R., Sposito, T., Steinmetz, R., Stevart, T., Suganuma, M.S., Sukri, R., Sultana, A.,
 762 Sukumar, R., Sunderland, T., Supriyadi, Suresh, H.S., Suzuki, E., Tabarelli, M., Tang, J., Tanner, E.V.J.,
 763 Targhetta, N., Theilade, I., Thomas, D., Timberlake, J., De Morisson Valeriano, M., Van Valkenburg,
 764 J., Van Do, T., Van Sam, H., Vandermeer, J.H., Verbeeck, H., Vetaas, O.R., Adekunle, V., Vieira, S.A.,
 765 Webb, C.O., Webb, E.L., Whitfeld, T., Wich, S., Williams, J., Wiser, S., Wittmann, F., Yang, X., Yao,
 766 C.Y.A., Yap, S.L., Zahawi, R.A., Zakaria, R. & Zang, R. (2018) Phylogenetic classification of the world's
 767 tropical forests. *Proceedings of the National Academy of Sciences of the United States of America*,
 768 **115**, 1837–1842.

769 Ter Steege, H., Pitman, N.C.A., Killeen, T.J., Laurance, W.F., Peres, C.A., Guevara, J.E., Salomão, R.P.,
770 Castilho, C. V, Amaral, I.L., de Almeida Matos, F.D. & others (2015) Estimating the global
771 conservation status of more than 15,000 Amazonian tree species. *Science advances*, **1**, e1500936.

772 Sullivan, M.J.P., Talbot, J., Lewis, S.L., Phillips, O.L., Qie, L., Begne, S.K., Chave, J., Cuni-Sanchez, A.,
773 Hubau, W., Lopez-Gonzalez, G., Miles, L., Monteagudo-Mendoza, A., Sonké, B., Sunderland, T., Ter
774 Steege, H., White, L.J.T., Affum-Baffoe, K., Aiba, S.I., De Almeida, E.C., De Oliveira, E.A., Alvarez-
775 Loayza, P., Dávila, E.Á., Andrade, A., Aragão, L.E.O.C., Ashton, P., Aymard, G.A., Baker, T.R., Balinga,
776 M., Banin, L.F., Baraloto, C., Bastin, J.F., Berry, N., Bogaert, J., Bonal, D., Bongers, F., Brienens, R.,
777 Camargo, J.L.C., Cerón, C., Moscoso, V.C., Chezeaux, E., Clark, C.J., Pacheco, Á.C., Comiskey, J.A.,
778 Valverde, F.C., Coronado, E.N.H., Dargie, G., Davies, S.J., De Canniere, C., Djuikouo, M.N., Doucet,
779 J.L., Erwin, T.L., Espejo, J.S., Ewango, C.E.N., Fauset, S., Feldpausch, T.R., Herrera, R., Gilpin, M.,
780 Gloor, E., Hall, J.S., Harris, D.J., Hart, T.B., Kartawinata, K., Kho, L.K., Kitayama, K., Laurance, S.G.W.,
781 Laurance, W.F., Leal, M.E., Lovejoy, T., Lovett, J.C., Lukasu, F.M., Makana, J.R., Malhi, Y.,
782 Maracahipes, L., Marimon, B.S., Junior, B.H.M., Marshall, A.R., Morandi, P.S., Mukendi, J.T.,
783 Mukinzi, J., Nilus, R., Vargas, P.N., Camacho, N.C.P., Pardo, G., Peña-Claros, M., Pétronelli, P.,
784 Pickavance, G.C., Poulsen, A.D., Poulsen, J.R., Primack, R.B., Priyadi, H., Quesada, C.A., Reitsma, J.,
785 Réjou-Méchain, M., Restrepo, Z., Rutishauser, E., Salim, K.A., Salomão, R.P., Samsøedin, I., Sheil, D.,
786 Sierra, R., Silveira, M., Slik, J.W.F., Steel, L., Taedoumg, H., Tan, S., Terborgh, J.W., Thomas, S.C.,
787 Toledo, M., Umunay, P.M., Gamarra, L.V., Vieira, I.C.G., Vos, V.A., Wang, O., Willcock, S. &
788 Zemagho, L. (2017) Diversity and carbon storage across the tropical forest biome. *Scientific*
789 *Reports*, **7**, 39102.

790 Tang, H., Dubayah, R., Swatantran, A., Hofton, M., Sheldon, S., Clark, D.B. & Blair, B. (2012) Retrieval of
791 vertical LAI profiles over tropical rain forests using waveform lidar at La Selva, Costa Rica. *Remote*
792 *Sensing of Environment*, **124**, 242–250.

793 Le Toan, T., Quegan, S., Davidson, M.W.J., Balzter, H., Paillou, P., Papathanassiou, K., Plummer, S., Rocca,
794 F., Saatchi, S., Shugart, H. & Ulander, L. (2011) The BIOMASS mission: Mapping global forest
795 biomass to better understand the terrestrial carbon cycle. *Remote Sensing of Environment*.

796 Watson, J.E.M., Darling, E.S., Venter, O., Maron, M., Walston, J., Possingham, H.P., Dudley, N., Hockings,
797 M., Barnes, M. & Brooks, T.M. (2016) Bolder science needed now for protected areas. *Conservation*
798 *Biology*, **30**, 243–248.

799 Watson, J.E.M., Evans, T., Venter, O., Williams, B., Tulloch, A., Stewart, C., Thompson, I., Ray, J.C.,
800 Murray, K., Salazar, A., McAlpine, C., Potapov, P., Walston, J., Robinson, J.G., Painter, M., Wilkie, D.,
801 Filardi, C., Laurance, W.F., Houghton, R.A., Maxwell, S., Grantham, H., Samper, C., Wang, S.,
802 Laestadius, L., Runting, R.K., Silva-Chávez, G.A., Ervin, J. & Lindenmayer, D. (2018) The exceptional
803 value of intact forest ecosystems. *Nature Ecology and Evolution*, **2**, 599.

804 Wolf, J.A., Fricker, G.A., Meyer, V., Hubbell, S.P., Gillespie, T.W. & Saatchi, S.S. (2012) Plant species
805 richness is associated with canopy height and topography in a neotropical forest. *Remote Sensing*,
806 **4**, 4010–4021.

807

808 **Data Availability Statement**

809 Most of the field and lidar data used in this study are available and can be downloaded directly from the
810 internet. Otherwise the datasets can be requested as described below. We have grouped the data in
811 four groups: (i) LVIS lidar data, (ii) ALS lidar data, (iii) field data and (iv) GEDI lidar data.

812 **(i) LVIS lidar data**

813 The LVIS data for the *rab*, *lop*, *mon* and *mab* study sites can be downloaded from the NASA data archive
814 at the following DOI: <https://doi.org/10.3334/ORNLDAAAC/1591>.

815 The LVIS data for the *cha* and *lsv* study sites is available on the following website:
816 <https://lvis.gsfc.nasa.gov/Data/Maps/CR2005Map.html>.

817 **(ii) ALS lidar data**

818 The ALS data over *rob* is available through the auscover data portal
819 ftp://gld.auscover.org.au/airborne_validation/lidar/robsons_creek/.

820 The ALS data over *s11* and *s12* can be downloaded from the sustainable landscapes data portal
821 <http://www.paisagenslidar.cnptia.embrapa.br/webgis/>.

822 The ALS data over *yan* and *mal* is available through ArcGIS online at
823 <https://www.arcgis.com/home/item.html?id=a6095e77541d4ad88dc6f0945639d089>.

824 The ALS data over *bci* is can be downloaded directly using the following download link:
825 http://www.life.illinois.edu/dalling/lidar_data.tgz.

826 The ALS data over *tam* is not publicly available online as it is actively supporting external research
827 projects. However, anyone interested in working with this data can contact Chris Hopkinson
828 (c.hopkinson@uleth.ca) or Ross Hill (rhill@bournemouth.ac.uk) to request access.

829 The ALS data over *dan* and *sep* is currently in the process of being made available through the Centre for
830 Environmental Data Analysis (CEDA) <https://www.ceda.ac.uk/>.

831 **(iii) Field data**

832 Field data from *rob* has been published through the Terrestrial Ecosystem Research Network (TERN)
833 data portal linked from <https://supersites.tern.org.au/supersites/fnqr-robson>.

834 The *dan*, *rab* and *bci* field data are all available on request through the Forestgeo website at
835 <https://forestgeo.si.edu/explore-data>: [https://forestgeo.si.edu/explore-data/rabi-](https://forestgeo.si.edu/explore-data/rabi-termsconditionsrequest-form)
836 [termsconditionsrequest-form](https://forestgeo.si.edu/explore-data/barro-colorado-island-termsconditionsrequest-forms), [https://forestgeo.si.edu/explore-data/barro-colorado-island-](https://forestgeo.si.edu/explore-data/barro-colorado-island-termsconditionsrequest-forms)
837 [termsconditionsrequest-forms](https://forestgeo.si.edu/explore-data/danum-valley-termsconditionsrequest-forms), [https://forestgeo.si.edu/explore-data/danum-valley-](https://forestgeo.si.edu/explore-data/danum-valley-termsconditionsrequest-forms)
838 [termsconditionsrequest-forms](https://forestgeo.si.edu/explore-data/danum-valley-termsconditionsrequest-forms).

839 The *sep*, *lop*, *tam* and *yan* field data are all available upon request through forestplots.net and can be
840 found under the project names ‘sepilok’, ‘lope’, ‘tambopata’ and ‘yangambi’ at
841 <https://www.forestplots.net/en/>.

842 The *mon* field data is archived through the NASA data archiving center and available at DOI:
843 <https://doi.org/10.3334/ORNLDAAAC/1580>.

844 The *s11* and *s12* were available through the data portals of the sustainable landscapes projects and can
845 be found under the field data from the São Félix do Xingu region collected in 2011 and 2012 in the
846 following data portal: <http://www.paisagenslidar.cnptia.embrapa.br/webgis/>.

847 The *cha* field dataset can be requested here <http://neoselvas.wordpress.uconn.edu/data/>.

848 The *lsv* data can be accessed through the following website: [https://tropicalstudies.org/carbono-](https://tropicalstudies.org/carbono-project/#1554994367217-6bb19222-75b7)
849 [project/#1554994367217-6bb19222-75b7](https://tropicalstudies.org/carbono-project/#1554994367217-6bb19222-75b7).

850 The *mab* field data are available through the following website: <https://github.com/umr->
851 [amap/centrafriplots](https://github.com/umr-).

852 The *mal* data are available upon request through <https://www.gfbinitiative.org/datarequest>.

853 **(iv) GEDI lidar data**

854 The different lidar data products from GEDI used to create figure 8 can be download through
855 https://doi.org/10.5067/GEDI/GEDI01_B.001, https://doi.org/10.5067/GEDI/GEDI02_A.001, and
856 https://doi.org/10.5067/GEDI/GEDI02_B.001.